C. R. Physique 3 (2002) 289–300

Solides, fluides: propriétés électroniques et optiques/*Solids, fluids: electronic and optical properties*
(Solides, fluides: structure/*Solids, fluids: structure*)

AGRÉGATS COMME PRÉCURSEURS DES NANO-OBJETS
CLUSTERS AS PRECURSORS OF NANO-OBJECTS

Mass selected cluster deposition in strongly or weakly interacting media

Wolfgang Harbich [*], **Christian Félix**

Institut de physique des nanostructures, Faculté des sciences de base, École polytechnique fédérale,
CH-1015 Lausanne, Switzerland

Received 20 February 2002; accepted 30 March 2002

Note presented by Guy Laval.

Abstract Mass selected cluster deposition is discussed with respect to three questions: what is the integrity of the clusters after deposition; are they uniform in terms of size and isomerisation; and finally what is the influence of the support on the clusters? The answer to these questions will depend on the strength of cluster media interaction and we have chosen two extreme cases the inert rare gases on one hand and metal surfaces on the other. Three examples are given: Raman studies as well as low-temperature STM give structural information on the deposited clusters, while other optical spectroscopies (absorption and fluorescence) yield information on the electronic structure of the clusters. ***To cite this article: W. Harbich, C. Félix, C. R. Physique 3 (2002) 289–300.*** © 2002 Académie des sciences/Éditions scientifiques et médicales Elsevier SAS

cluster deposition / softlanding / geometrical structure / electronic structure

Déposition d'agrégats triés en taille dans des milieux avec de fortes ou faibles interactions

Résumé La déposition d'agrégats sélectionnés en taille est discutée en rapport avec trois questions : quelle est l'inégrité des agrégats après la déposition, quelle est leur uniformité en terme de taille et d'isomérisation et finalement quelle est l'influence du support ? La réponse à ces questions dépendra de la force de l'interaction entre l'agrégat et le milieu dans lequel il se trouve. Nous avons choisi deux cas extrêmes : les gaz rares inertes d'un côté et des surfaces métalliques de l'autre. Trois exemples sont discutés : Des études des spectroscopie Raman ainsi que des mesures de microscopie tunnel donnent des informations de structure géométrique sur les agrégats déposés, alors que d'autres spectroscopies optiques (absoption et fluorescence) livrent des informations sur leur structure électronique. ***Pour citer cet article : W. Harbich, C. Félix, C. R. Physique 3 (2002) 289–300.*** © 2002 Académie des sciences/Éditions scientifiques et médicales Elsevier SAS

deposition d'agrégats / structure geométrique / structure electronique

---

[*] Correspondence and reprints.
E-mail addresses: wolfgang.harbich@epfl.ch (W. Harbich); christian.felix@epfl.ch (C. Félix).

S1631-0705(02)01320-8/FLA

1. Introduction

Softlanding of mass selected clusters has been formulated as a challenge since the beginning of cluster science. However, when we use the term “Mass Selected Cluster Deposition” (MCSD) we draw a rather flawed picture of the purpose of this research topic and this is so because MSCD is a technique rather than a research object in itself. Consequently, the motivation to perform MSCD is manifold and has changed in the last ten years.

The pioneering era on cluster research focused mainly on gas phase work [1]. It became evident that physical properties (as, for example, stability manifesting itself in mass spectra intensities) were depending strongly on the number of atoms of the cluster. In this context consider the famous shell structure for metal clusters where the stability of the particle is given by the number of valence electrons. These experiments were beam experiments in the early times of the development of cluster sources. For the most part of cluster materials and sizes, source intensities were and still are, very weak restricting the number of research tools. Concluding remarks in the ISSPIC (International symposium on Small Particles and Inorganic Clusters) conferences tended to be: we need information on electronic and geometric structure. However, vibrational spectroscopies which give access to structural properties of clusters were out of the scope at these low target densities. Optical spectroscopies were restricted to experiments such as laser induced fluorescence (LIF), resonant two photon ionisation (R2PI) but the most straightforward experiment (optical absorption) was not possible. For these reasons matrix isolation spectroscopy in rare gases on mass selected clusters became an important issue, since target densities which were several orders of magnitude higher could be accumulated. First results from Schulze and coworkers [2] showed the strength of this technique but it became immediately clear that for clusters larger than dimers one could not allow for a large size distribution in matrices which made mass selection imperative.

When people were speculating on the properties of small clusters, reactivity has been pushed forward as a possible candidate to look at. This became in particular evident after the publication of Rileys work on the hydrogen uptake of Fe clusters [3] in the gas phase. Rate constants were changing orders of magnitude by adding just one atom to the cluster. These experiments have recently found their counterpart in metal clusters deposited on metal oxide surfaces approaching, as model systems, the real world of catalysis [4]. Together with ab initio calculations deep insight into the mechanisms of catalysis have been obtained. Here again the controlled deposition of the clusters in size and energy were a key step for the success.

We discuss mass selected cluster deposition in the context of three questions: what is the integrity of the clusters after deposition; are they uniform in terms of size and isomerisation; and finally what is the influence of the support on the clusters? Selected examples of the work of the authors are presented to try to give an answer to these questions. Basically two question are addressed, geometrical and electronic structure, which depend on each other. Novel properties will be expected from the discreteness of the electronic levels with respect to the bandstructure formation in solids. This can be, in particular, interesting for metals, since a bandgap can arise at the very small sizes.

2. Deposition process

The production of clusters, their mass selection and finally their deposition on a well defined substrate still is a technically very challenging experiment. Later, when the deposition has been accomplished we need a means to probe the surface or the thin film and to identify the resulting cluster substrate morphology. Although size specific results have been obtained, for example, in catalytic experiments (see above) [4,5], the identification of cluster size and morphology after deposition is still a bottleneck, and so far only STM work from our group gives conclusive results which will be presented later. The technical aspects of mass selected cluster deposition are far from being routine and will be discussed briefly followed by experimental results about fragmentation and implantation.

2.1. Technical aspects

Mass selected cluster deposition requires a cluster source, a beam line with a mass filtering device and a support to deposit the cluster. Normally this will be a surface science experiment operating under ultra high vacuum conditions. In most cases the substrate has to be cooled in order to stabilize the cluster morphologies which are, since they are very small, fragile.

(a) Cluster source: Cluster deposition needs intense, custom made cluster sources. The most prominent ones are sputter sources [6–9] and Laser vaporisation sources (LVPS) [10]. LVPS have been improved quite considerably in the last years and have become superior to sputter sources for larger cluster sizes although they are pulsed in nature.

(b) The mass selection device is almost exlusively a quadrupole mass filter because of the high transmission and variable resolution over a convenient mass range (typically 1–10000 amu).

A mass spectrum of silver clusters taken from a sputter source is given in Fig. 1. Typically 0.5–1.5 nA of mass selected clusters can be obtained. The beam size is 3–4 mm FWHM. This number can serve as a yardstick for today's employed cluster sources for mass selected deposition. The number given translates in a deposition time of typically 1 hour for a monolayer equivalent of deposited material. In most practical cases deposition times are much shorter since far less than a monolayer is needed.

Deceleration of the cluster beam is normally necessary for a softlanding experiment since the beam is transported at higher kinetic energies for better transmission. The minimum deposition energy which can be achieved depends strongly on the type of cluster source. LVPS has an intrinsic energy width which is small and landing energies of $E_{\mathrm{kin}} < 1$ eV can be obtained. This is different in sputter sources where the intrinsic energy width does not allow us to decelerate the cluster below a kinetic energy of about 10 to 15 eV unless the cluster ions are thermalized by collisions with rare gas atoms in a so called phase space compressor [11,12].

The deposition and analysis chamber is unique to the the different types of experiments which will be performed. More or less detailed descriptions can be found in the literature [9,10,13].

2.2. Softlanding and hardlanding

The possible outcome of the cluster deposition process [14] is rich and will not be discussed in detail. However, two main directions are investigated right now. The softlanding which aims to keep the cluster intact upon landing and implantation where a certain amount of energy is given to a cluster to allow it to penetrate into the surface and form that way a thermally much more stable morphology. In the

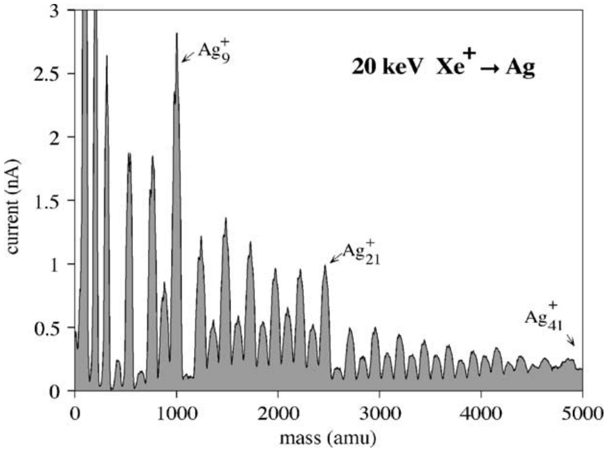

Figure 1. Mass spectrum taken from a sputter source used in our group.

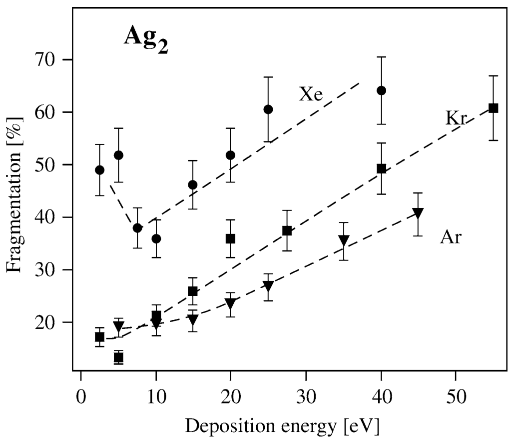

Figure 2. Fragmentation F of Ag_2 as a function of impact energy in Ar, Kr and Xe.

case of softlanding, the constraints are clear: slow down the particle as much as possible in order to avoid fragmentation. However, one has to keep in mind that the cohesive energy between substrate and particle leads to a considerable acceleration. Molecular dynamics simulations for example suggest [15] that implantation of Ag clusters in Pd(100) is possible at zero kinetic deposition energy. As the cluster substrate interaction becomes weak, this acceleration is strongly suppressed. Further, if we employ rare gas substrates, the 'soft' nature of the support supplies an efficient energy absorber for the remaining kinetic energy and almost fragmentationless deposition can be achieved even at 10 to 20 eV kinetic deposition energy [16]. Figure 2 shows the fragmentation of Ag dimers in different rare gas matrices from which it becomes clear that the softer the matrix the smaller the fragmentation. This phenomenon is responsible for the fact that matrix isolation on mass selected cluster has become an important spectroscopic tool (see below).

Our group as well as the group of Wurth have used this pillow effect to perform softlanding experiments on stronger interacting surfaces in the following way. Prior to deposition an ultrathin (typically some 10 monolayers) layer of rare gas is adsorbed on the surface. After deposition the 'pillow' is desorbed by gently heating the matrix forcing the cluster to reach the surface in thermal equilibrium with its surrounding [17,9]. This type of experiment is the basis for the structural investigation in Section 4.

3. Structural properties

For small systems there is a strong interaction between geometric and electronic structure. In order to understand, to compare with theory and ultimately to tweak the electronic properties of metal clusters on a support, it is essential to have a precise idea of their geometrical structure.

Depending on the system studied the techniques will vary; however, we can summarize the available techniques for neutral clusters in two categories:

(a) Spectroscopy techniques like Raman or IR-spectroscopy, which yield vibrational information. But more electronic oriented spectroscopies such as absorption or fluorescence can also yield geometric information. We would like to emphasize here that these spectroscopic techniques require the comparison with state of the art ab initio calculations. It is this comparison that really yields information;

(b) In the case of clusters deposited on a substrate, local probe spectroscopy techniques like STM, or AFM deliver a real space image and therefore a detailed geometric characterization.

To illustrate these studies we will concentrate in the following on two examples; the first dealing with clusters in a matrix and the second with surface deposited clusters.

3.1. Matrix isolated clusters: resonant Raman spectroscopy

The geometrical structure of clusters is going to be affected by the presence of the solid matrix around it. By choosing as matrix a condensed and relatively inert gas, we expect the interaction with the substrate to be low, and therefore the cluster geometrical structure to be close to the structure in the gas phase. An important question is: how low is the interaction going to be?

As discussed above (see Section 2), clusters can be deposited in a gas matrix while avoiding most of the fragmentation, provided that their deposition energy is sufficiently small (typically in the order of a few eV/atom) [18]. In the case of carbon clusters, absorption spectra have been measured for small sizes by Maier and coworkers showing that the fragmentation was negligible.

To illustrate the methods used to identify the structure, we will concentrate on a neutral carbon cluster: C_{20} in an N_2 matrix. C_{20}^+ ions are mass selected and co-deposited with ultra-pure N_2 under UHV conditions, in order to create a seeded matrix. A filament produces the neutralizating electrons.

C_{20} has been proposed as possibly the smallest fullerene [19,20] and a precursor to formation of fullerene C_{60} [21,22]. C_{20} has several isomers with approximately the same energies, including the linear chain, the monocyclic ring, the corranulene-like bowl, and the fullerene cage (Fig. 3). Much experimental information

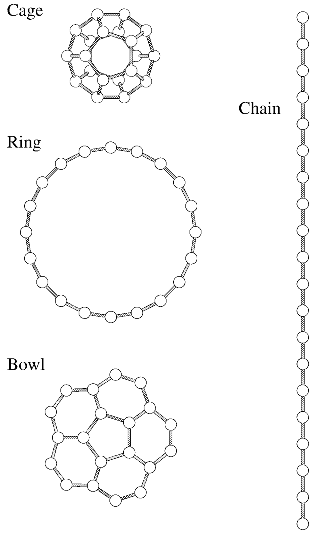

Figure 3. C_{20} has several isomers with approximately the same energies, including the linear chain, the monocyclic ring, the corranulene-like bowl, and the fullerene cage.

is available for cluster ions: C_{20}^{+} is known to have a ring structure while C_{20}^{-} is known to be linear. Experimental measurements on neutral carbon clusters are scarce (see Ref. [23] and references therein); in particular, nothing was known on neutral C_{20}.

Raman spectroscopy typically yields vibrational information, the problem lies in the usually very low cross sections for this phenomenon. Since the mass selected cluster source does not deliver macroscopic amounts of material, the signal needs to be enhanced. Surface Enhanced Raman Scattering (SERS) allows for a huge enhancement (up to a factor 10^6) of the Raman signal, but it requires the particle to be in contact or at least be very close to a rough silver surface. The interaction with the surface may influence the structure of the clusters and was therefore avoided. An alternative technique called Surface Plasmon–Polariton (SPP) enhanced Raman spectroscopy (enhancement factor $\sim$100) [24] was used to gain information on the structure of size selected clusters. When the excitation energy of the laser is close to the energy difference between the ground state and an excited state, the Raman signal can be resonantly enhanced. The enhancement factor can be in the order of 10^5. The drawback, however, is that the selection rules that forbid the combinations and overtones in normal Raman Scattering (RS) are broken. The interpretation of the experimental lines is therefore more difficult. To extract the fundamental vibrational modes from the Raman measurements, we had to look for the common features at many excitation wavelengths.

In Fig. 4 the fundamental vibrational wavelengths extracted from the experiment are compared to calculated Raman spectra from the different C_{20} possible structures [23]. The spectra were calculated with density functional theory, using the B3LYP (Becke three-parameter Lee–Yang–Parr) functional [25] and the cc-pVDZ (correlation consistent polarized valence double zeta) basis set [26]. The B3LYP/cc-pVDZ harmonic frequencies were uniformly scaled down by 2% to account for the systematic overestimation that results from the neglect of anharmonic effects (see [23] for details).

From this comparison, we see that the experimental vibrations do not match with the calculated spectrum for the cage structure: Raman lines are observed at energies higher than 2000 cm^{-1} that are typical of triple carbon bonds. These triple bonds do not exist in a fullerene-like structure. We can therefore exclude the cage type structure. Similarly the ring structure can be excluded, since a vibration is observed around 1500 cm^{-1}, while such a vibration does not exist in rings.

The last candidate structures are either the bowl or the linear chain. Comparison of the Raman signal for C_{16}, C_{18} and C_{20} shows similarities in the spectra. This alone points towards a structure that is scalable like linear chains or rings and therefore excludes the bowl structure. A systematic shift towards lower frequencies is observed for increasing sizes, as reported in Table 1.

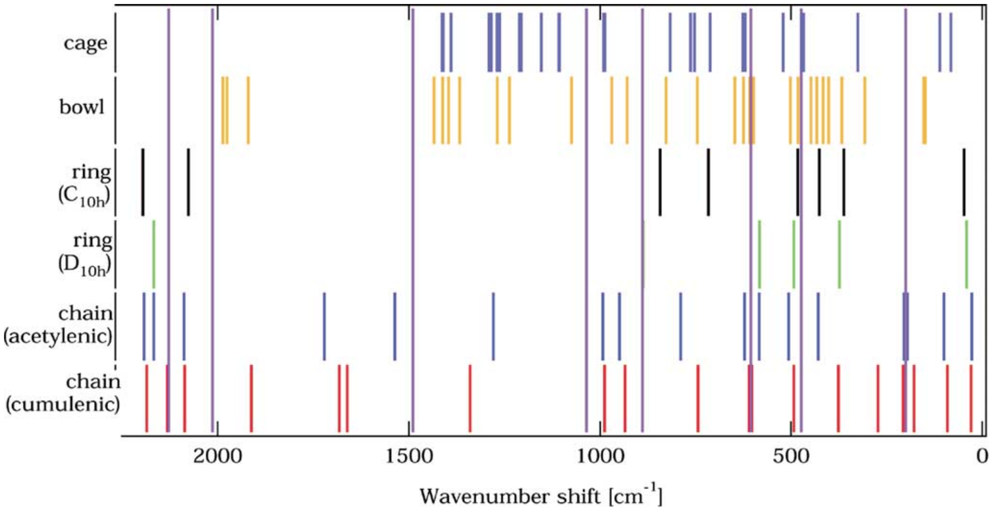

Figure 4. Calculated vibrational frequencies that Raman active (short vertical lines) for different possible structures of C_{20} are compared to the measured fundamental vibrational frequencies (long vertical lines).

Table 1. Systematic shift of a vibration with increasing size of the carbon cluster

	Exp. freq.	Cumulene chain freq.	Acethylenic ring freq.
C_{16}	249	258	260
	735	752	538
C_{18}	223	230	320
	650	674	653
C_{20}	200	207	363
	605	609	716

The agreement with the linear chain is very good. The values for acethylenic rings are given as an additional prove that we do not observe rings in our samples.

Although the existence of linear chains is indicated by the data, the ring is the dominant isomer for C_{20}^{+} clusters in the gas phase [27,28]. The deposited clusters must, therefore, convert from rings to chains upon neutralization. The ionization potentials of C_{20} is approximately 8 eV [29], and neutralization of the clusters could provide enough energy to break apart the rings to form chains. A further possibility is that both rings and chains exist in the sample, but that the resonance Raman effect is much stronger for the chain structures, thereby making the chain fundamentals the dominant features of the spectra.

Therefore in the question of structural uniformity, we have proven the existence of linear chains for neutral C_{20} in matrices, but we have not yet proven its unicity. The interaction with the support has not really been addressed directly, but the good agreement of the calculated spectra with the experiments indicates that this interaction is low.

3.2. Clusters on surfaces: STM studies

When clusters get into contact with strongly interacting surfaces we will expect that the shape will change from the gas phase or the rare gas morphology. While a 19 atom metal cluster has an almost spherical shape in the gas phase governed by the electronic system [30], the contact with a metal surface will decrease the total energy by forming metal bonds between the cluster and the surface atoms. Intuitively (and also

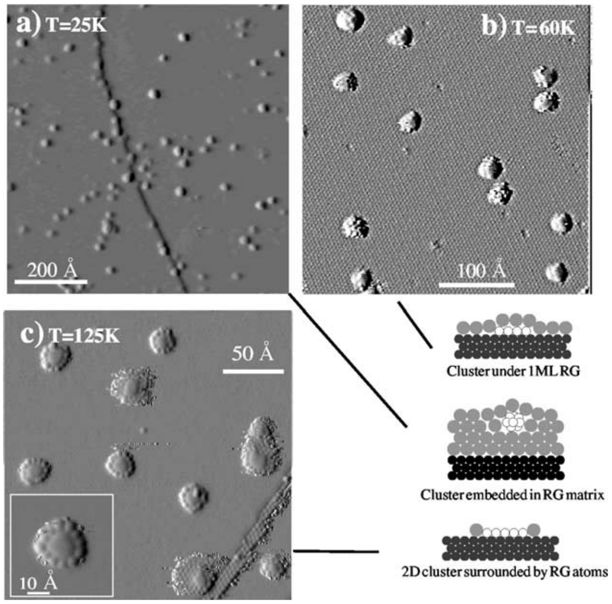

Figure 5. Cluster-substrate morphology with the corresponding STM images for Ag_{19}/Kr/Pt(111) at different annealing temperatures. Also given are cartoons illustrating the proposed morphologies.

confirmed by density functional calculations [31]) we will expect for a Ag_{19} cluster on a Pt(111) surface a regular hexagon with monoatomic height, since silver grows layer by layer on Pt(111) [32].

In the following paragraph we discuss this system briefly in the context of the three questions raised above: integrity, interaction with the support and structure uniformity.

In order to verify the hexagonal shape we have to perform a softlanding experiment on a strongly interacting surface. This is done using the rare gas layer buffer technique as described above, in this case a thin layer of Kr. After cluster deposition we gently heat the matrix in order to evaporate the rare gas matrix. Figure 5 show STM pictures after deposition of Ag_{19} at different surface temperatures. The corresponding morphologies are depicted in the cartoon like pictures in the same figure. Directly after deposition at $T_s = 25$ K we find the cluster embedded in the buffer layer. For further investigations we make use of the different binding energies of Krypton atoms placed in different environments. This allows us to desorb them selectively. At an annealing temperature of $T_s = 60$ K the Kr atoms, which are bound to other Kr atoms, desorb, while the Kr atoms in contact with the Pt terraces, steps, or Ag clusters do not. This situation is shown in Fig. 5(b), where the Pt terraces and clusters are covered with one monolayer of Kr. It is imaged on Pt(111) with atomic resolution. The Ag_{19} clusters are imaged as protrusions with lateral dimensions which correspond well to a rare gas covered 2D or 3D cluster as depicted in the cartoon in Fig. 5.

Further annealing results in evaporation from the terraces leaving only higher coordinated Kr atoms at steps. The Kr atoms form a chain along the step edges and a ring around the adsorbed clusters. The same situation is obtained by desorbing completely the Kr overlayer and redepositing a small amount of Kr, just sufficient to decorate the step edges and the clusters. This is the situation measured in Fig. 5(c) for $T_s = 125$ K during redeposition of Kr atoms. The monoatomic steps of the Pt(111) surface as well as the adclusters are decorated by Kr atoms.

Figure 6 gives more detailed information on the Ag cluster decorated by a ring of Kr atoms shown in the inset of Fig. 5(c). The high resolution STM image of this cluster clearly shows that it is surrounded by 12 Kr atoms. A line scan across the particle as shown in Fig. 6(b) reveals the ‘electronic height’ of Ag on Pt.

It is unfortunately not possible to find atomic resolution for the Ag atoms themselves; however, the Kr decoration allows us to find, in an indirect way, the size and shape of the Ag island. As described in more

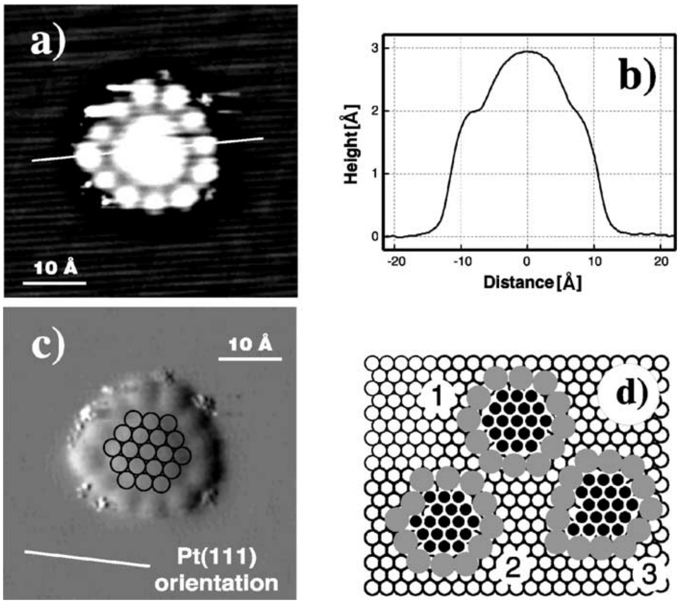

Figure 6. Ag_{19} cluster on Pt(111) surrounded by 12 Kr atoms. (a) $I = 380$ pA, $V_{\text{bias}} = -200$ mV; the image has been filtered to artificially increase the contrast; (b) linescan across the cluster; (c) model superposed to the image; (d) models for different adcluster morphologies.

detail in [33] and as shown in Fig. 6(c), one can place exactly 12 Kr atoms around a 19 atom hexagon (Fig. 6(d)). The Kr necklace is sensitive to the shape of the island. For example model 3 corresponds to a 19 atoms island with an irregular shape: 13 Kr atoms are needed. However, this choice is not unique in the sense that the configuration 2 in Fig. 6(d) would not be necessarily distinguishable from configuration 1. The observation that most clusters reach an equilibrium shape means that either the energy barrier for a transition from an irregular to a regular shape is small, or that the ‘shape energy’, which is released when the cluster comes into contact with the surface [15], allows the cluster to transform immediately into its energetically favorable form. We believe that the latter is true since it has been shown [32] that a structural change of the cluster by edge diffusion is frozen at the temperatures considered. That only about 70% of the clusters show a 12 atoms ring arises from incompleted dressing of the cluster and from fragmentation into smaller clusters.

The hexagonal morphology of a 19 Ag atoms island is further supported by the following experiment. We first raise the temperature of the substrate to 140 K, in order to evaporate all Kr atoms, and then redeposit Kr during cooldown. We expect that during redeposition the rare gas atoms move freely on the Pt surface, first attach to the metallic step edges (this is the situation of Fig. 6(c), and when these are saturated attach to the step edges formed by the condensed rare gas and gradually build a full monolayer. At the same time Kr atoms condense on top of the 2D silver islands, adjusting themselves in a minimum energy configuration. This is the experiment described in Fig. 7. The Kr monolayer on top of Pt(111) together with some Ag clusters is shown in Fig. 7(a), a magnification of one of the clusters is given in Fig. 7(b). Seven Kr atoms forming a centered hexagon are accommodated on top of a Ag island. We also observe that the hexagon is rotated by about 7 degrees compared to the crystallographic direction of Pt(111). These observations can be nicely explained within a simple hard sphere model. We assume that the 19 atoms island has the shape of a regular hexagon and place the KR atoms at the minimum energy position on top of the island. One then easily realizes that the hexagon can only accommodate 7 Kr atoms, and that the Kr overlayer should be rotated by approximately 10 degrees with respect to the substrate. Such a model is shown in Fig. 7(c). If we remove an atom from the Ag hexagon, the Kr heptamer on the Ag_{19} terrace becomes very unlikely, since one of the 7 Kr atoms would not be in a stable configuration. This removes the ambiguity between the configurations (1) and (2) of Fig. 6(d).

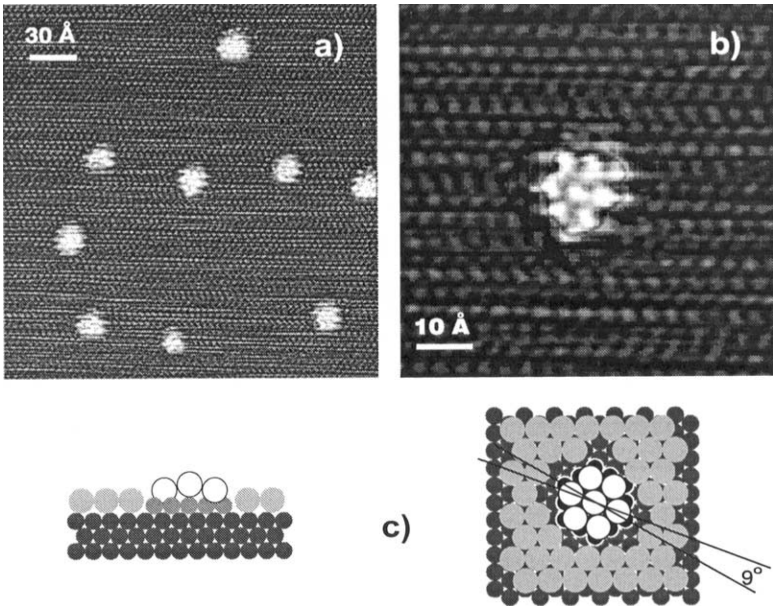

Figure 7. Kr redeposited on top of Ag_{19}: (a) overview $I = 430$ pA, $V_{\text{bias}} = -210$ mV; (b) zoom in; (c) proposed model.

This example is particular since the three questions raised above: integrity, interaction with the support and structure uniformity are answered and shown in Fig. 6(a). We have prepared a sample with (neglecting a small amount of fragmentation) a unique size. It should be stressed at this point that not only we have a monodispersed sample with respect to size but also with a unique shape, i.e. we have basically one isomer which is in the energetic ground state.

4. Electronic properties

Clusters lie at the limit of two classical fields of research: solid state physics and molecular physics. Therefore the models that are used for the description of these objects use both descriptions.

Numerous studies have been made to understand the electronic properties of metal clusters (see [30,34] for reviews on this subject). For big particles ($n \geqslant 100$) the theory of Mie describes the optical properties of metal clusters in a surrounding medium adequately. For smaller sizes, most of the observed electronic features near the Fermi level were interpreted with the prevalent model for the electronic structure of metal clusters: the particle-in-a-box shell model. In particular for silver clusters size selective absorption spectra have been measured in the gas phase [35] and isolated in rare gas matrices [36,37].

Gas phase experiments on Na_n clusters by Haberland and coworkers [38,39] have shown that, if the clusters are sufficiently small and sufficiently cold, their electronic response is molecular-like, otherwise their response is more jellium-like. This transition is interpreted as inhomogeneous broadening effects arising with increasing temperature. In the rare gas matrix isolation experiments the temperature of the clusters can be kept low enough so that the temperature broadening effects are negligible.

The interest of small metal clusters is therefore that they exhibit quantum confinement effects that can be understood by a simple model, even at very small sizes. This small size regime allows us to use our size-selective deposition technique to produce samples that are mono-dispersed and to study the size specificity of their electronic properties.

4.1. Fluorescence

It is only in recent experiments that the fluorescence of metal clusters bigger than a trimer has been observed (Ag_4 in Ar [40], Ag_8 in Ar [41] and indications of others [42]). Another group has reported

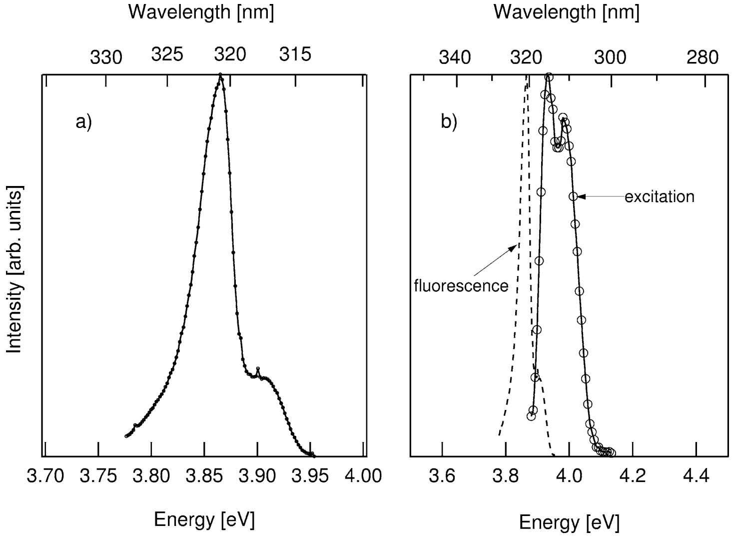

Figure 8. (a) Fluorescence spectrum of Ag_8 in an Ar matrix. Excitation energy: 3.98 eV; (b) Corresponding excitation spectrum.

a very broad fluorescence in gold nanocrystals (Au_{20}, Au_{38}, Au_{135} surrounded by a passivating layer of dodecanethiol molecules [43]) that they tentatively attribute to gold 6_{sp} intraband transitions. In somewhat bigger gold nanocrystals ($n \geqslant 1000$) s to d interband transitions have been reported [44].

Figure 8(a) shows the fluorescence spectrum of Ag_8 in an argon matrix. The fluorescence has two main peaks, one centered at 3.87 eV and a second centered at 3.90 eV. The peaks are narrow (36 meV FWHM) compared to the fluorescence of small metal molecules like dimers and trimers [45,46].

Contrary to semiconductors, metals do not have a band gap and therefore luminescence from metal surfaces, for example, has a very low efficiency. Semiconductors have an energy gap that does not disappear with the formation of the band structure. Metal clusters on the contrary have a HOMO-LUMO gap only as long as they are sufficiently small; the formation of the band structure kills the energy gap. Luminescence can only be efficient if an energy gap is present, therefore it will be important only for very small metal particles.

4.2. Matrix effects

The surrounding matrix is going to have a considerable effect on the fluorescence of the embedded clusters. Two phenomena, the cage effect and the vibrational coupling, give opposite contributions and it is the balance between those that will determine the fluorescence yield of the metal clusters.

Gas phase experiments have shown for metals clusters that the fragmentation upon absorption of a photon was very rapid: ~ 5 ps for K_3 [47]. This is shorter than the time necessary for dipolar transitions and therefore no fluorescence can be observed in that case. The presence of a surrounding matrix prevents the clusters from dissociating and permits a long enough lifetime of the particle for the fluorescence to be observed. This is known as the ‘cage effect’.

Another important effect of the medium is vibrational relaxation. A small molecule in the gas phase when placed into a vibrationally excited level will, in the absence of collisions, remain in that level and can only return to the ground state by a radiative process. However, a solid matrix can act as an effective energy sink and vibrational relaxation can occur and, in fact, does occur even for small molecules [48]. There are molecules where the fluorescence, which is prominent in the gas phase, may be completely quenched in the matrix [48,49].

The excitation spectrum corresponding for the fluorescence reported in Fig. 8(a) is shown in Fig. 8(b). It is recorded by monitoring the intensity of the main fluorescence peak while scanning the excitation wavelength. The excitation lies very close to the fluorescence. Recent ab initio calculations [50] are in very

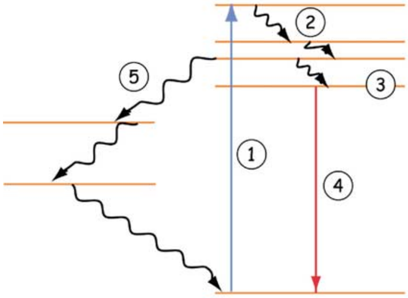

Figure 9. Scheme for the the excitation dynamics of a small metal cluster. Once excited (1) the cluster relaxes through vibrational coupling (2) to the matrix to the lowest available excited state (3). From there the energy gap to the ground state is too large for the vibrational coupling to be efficient and therefore the fluorescence (4) is possible. Competitive relaxation (5) through other channels may be present.

good agreement with these measurements and suggest that the fluorescence results from the 5 $^1T_2$ of the T_d structure of Ag_8. In particular the calculations also show a Stokes shift of 0.2 eV for the fluorescence. Note that the excitation spectrum is an isomer selective information.

For neutral molecules, the position of the peaks are slightly shifted due to interactions with the matrix [48] for Ag_n in argon the shift is typically 0.25 eV compared to the gas phase value [51].

Figure 9 shows an energy scheme for what we think is the excitation dynamics that allows for the observed fluorescence. The model proposed here is very similar to what happens in semiconductors where a phonon mediated relaxation happens down to the lower edge of the conduction band. Here the relaxation happens also via vibrational coupling but between close lying excited states. As long as the metal clusters are sufficiently small, the band structure is not yet formed and the metal clusters have to be considered more like semiconductor nanoparticles.

5. Conclusions

Mass selected cluster deposition onto an inert substrate serves to study the intrinsic properties of clusters. UV-visible as well as Raman spectroscopy for matrix isolated particles have been and are very powerful for the study of molecules and radicals. Although these optical techniques have been applied to clusters from the early beginning of cluster spectroscopy, serious difficulties due to the inherent size distributions in conventionally prepared matrices arose. Mass selection combined with softlanding has allowed to make a big step forward. As shown and discussed here structural as well as electronic properties could be determined.

Mass selected deposition on surfaces to produce well defined nano or even Angström structures are still in the beginning but already spectacular results, for example, in catalysis have been obtained and it becomes evident from these studies that a detailed understanding and comparison to theory makes it necessary to know the number of atoms forming the cluster as well as morphology. The influence of the cluster substrate interaction becomes evident in the examples discussed and first successful experiments have been performed on strongly interacting substrates revealing the morphologies as well as the stability of the cluster substrate system.

Acknowledgements. The authors are deeply indebted to Prof. Jean Buttet the head of our group who constantly encouraged us to pursue this research direction. We dedicate this article to him on the occasion of his emeritation in March 2002.

References

[1] Proccedings of ISSPIC IV, Berlin, 1984, Springer-Verlag, Berlin, Heidelberg, New York, 1984.
[2] W. Schulze, H. Becker, H. Abe, Chem. Phys. 35 (1978) 177.
[3] E. Parks, B. Weiller, P. Bechthold, W. Hoffmann, G. Niemann, L. Pobo, S. Riley, J. Chem. Phys. 88 (1988) 1622.
[4] A. Sanchez, S. Abbet, U. Heiz, W.D. Schneider, H. Hakkinen, R.N. Barnett, U. Landman, J. Phys. Chem. A. 103 (1999) 9573.

[5] P. Fayet, F. Granzer, G. Hegenbart, E. Moisar, B. Pischel, L. Woste, Phys. Rev. Lett. 55 (1985) 3002.
[6] P. Fayet, L. Wöste, Surf. Sci. 156 (1985) 134.
[7] H.V. Roy, P. Fayet, F. Patthey, W.D. Schneider, B. Delley, C. Massobrio, Phys. Rev. B 49 (1994) 5611.
[8] C. Felix, G. Vandoni, C. Massobrio, R. Monot, J. Buttet, W. Harbich, Phys. Rev. B 57 (1998) 4048.
[9] J.T. Lau, A. Achleitner, W. Wurth, Chem. Phys. Lett. 317 (2000) 3.
[10] U. Heiz, F. Vanolli, L. Trento, W.D. Schneider, Rev. Sci. Instrum. 68 (1997) 1986.
[11] T. Leisner, C. Rosche, S. Wolf, F. Granzer, L. Woeste, Surf. Rev. Lett. 3 (1996) 1105.
[12] K.J. Boyd, A. Lapicki, M. Aizawa, S.L. Anderson, Rev. Sci. Instrum. 69 (1998) 4106.
[13] H. Jodicke, R. Schaub, A. Bhowmick, R. Monot, J. Buttet, W. Harbich, Rev. Sci. Instrum. 71 (2000) 2818.
[14] W. Harbich, in: K.H. Meiwes-Broer (Ed.), Collision of Clusters with Surfaces: Deposition, Surface Modifications and Scattering, Springer-Verlag, Berlin, 2000.
[15] B. Nacer, C. Massobrio, C. Felix, Phys. Rev. B 56 (1997) 10590.
[16] S. Fedrigo, W. Harbich, J. Beljaev, J. Buttet, Chem. Phys. Lett. 211 (1993) 166.
[17] K. Bromann, C. Felix, H. Brune, W. Harbich, R. Monot, J. Buttet, K. Kern, Science 274 (1996) 956.
[18] S. Fedrigo, W. Harbich, J. Buttet, Phys. Rev. B 58 (1998) 7428.
[19] B.N. Cyvin, E. Brendsdal, J. Brunvoll, S.J. Cyvin, J. Mol. Struct. 352/353 (1995) 481.
[20] V. Parasuk, J. Almlöf, Chem. Phys. Lett. 184 (1991) 187.
[21] C.J. Barbec, E.B. Anderson, B.N. Davidson, S.A. Kajihara, Q.-M. Zhang, J. Bernholc, D. Tomanek, Phys. Rev. B 46 (1992) 7326.
[22] H.W. Kroto, K. McKay, Nature 331 (1988) 328.
[23] A.K. Ott, G.A. Rechtsteiner, C. Felix, P. Hampe, M.F. Jarrold, R.P. Van Duyne, K. Raghavachari, J. Chem. Phys. 109 (1998) 9652.
[24] E.C. Honea, A. Ogura, D.R. Peale, C. Félix, C.A. Murray, K. Raghavachari, W.O. Sprenger, M.F. Jarrold, W.L. Brown, J. Chem. Phys. 110 (1999) 12161.
[25] A.D. Becke, J. Chem. Phys. 98 (1993) 5648.
[26] T.H.J. Dunning, J. Chem. Phys. 90 (1989) 1007.
[27] G. von Helden, M.-T. Hsu, N. Gotts, M.T. Bowers, J. Phys. Chem. 97 (1993) 8182.
[28] K.B. Shelimov, J.M. Hunter, M.F. Jarrold, Int. J. Mass Spectrom. Ion Processes 138 (1994) 17.
[29] S.B.H. Bach, J.R. Eyler, J. Chem. Phys. 92 (1990) 358.
[30] W.A. de Heer, Rev. Mod. Phys. 65 (1993) 611.
[31] H. Parks, Private communication.
[32] H. Brune, Surf. Sci. Rep. 31 (1998) 121.
[33] R. Schaub, H. Jödicke, F. Brunet, R. Monot, J. Buttet, W. Harbich, Phys. Rev. Lett. 86 (2001) 3590.
[34] U. Kreibig, M. Vollmer, Optical Properties of Metal Clusters, Springer Series in Material Science, Vol. 25, Springer, Berlin, 1995.
[35] J. Tiggesbaumker, L. Koller, K.H. Meiwes Broer, A. Liebsch, Phys. Rev. A 48 (1993) R1749.
[36] W. Harbich, S. Fedrigo, J. Buttet, Chem. Phys. Lett. 195 (1992) 5.
[37] W. Harbich, S. Fedrigo, J. Buttet, Z. Phys. D 26 (1993) 138.
[38] C. Ellert, M. Schmidt, C. Schmitt, T. Reiners, H. Haberland, Phys. Rev. Lett. 75 (1995) 1731.
[39] C. Ellert, M. Schmidt, T. Reiners, H. Haberland, Z. Phys. D 39 (1997) 317.
[40] C. Félix, C. Sieber, W. Harbich, J. Buttet, I. Rabin, W. Schulze, G. Ertl, Chem. Phys. Lett. 313 (1999) 105.
[41] C. Félix, C. Sieber, W. Harbich, J. Buttet, I. Rabin, W. Schulze, G. Ertl, Phys. Rev. Lett. 86 (2001) 2992.
[42] I. Rabin, W. Schulze, G. Ertl, J. Chem. Phys. 108 (1998) 5137.
[43] T.P. Bigioni, R.L. Whetten, O. Dag, J. Phys. Chem. B 104 (2000) 6983.
[44] J.P. Wilcoxon, J.E. Martin, F. Parsapour, B. Wiedenman, D.F. Kelley, J. Chem. Phys. 108 (1998) 9137.
[45] P.S. Bechthold, U. Kettler, W. Krasser, Surf. Sci. 156 (1985) 875.
[46] S. Fedrigo, W. Harbich, J. Buttet, J. Chem. Phys. 99 (1993) 5712.
[47] H. Ruppe, S. Rutz, E. Schreiber, L. Wöste, Chem. Phys. Lett. 257 (1996) 3.
[48] V.E. Bondybey, T.A. Miller, in: T.A. Miller, V.E. Bondybey (Eds.), Molecular Ions: Spectroscopy, Structure and Chemistry, North-Holland, Amsterdam, 1983.
[49] M. Jacox, J. Phys. Chem. Ref. Data 27 (1998) 115.
[50] V. Bonacic-Koutecky, V. Veyret, R. Mitric, J. Chem. Phys. 115 (2001) 10450.
[51] W. Harbich, Y. Belyaev, R. Kleiber, J. Buttet, Surf. Rev. Lett. 3 (1996) 1147.